

Spring 2016

# A feasibility study of a nuclear power plant with no moving parts

Jonathan Mark Schattke

Follow this and additional works at: [http://scholarsmine.mst.edu/masters\\_theses](http://scholarsmine.mst.edu/masters_theses)

 Part of the [Nuclear Engineering Commons](#), and the [Plasma and Beam Physics Commons](#)

**Department:**

---

## Recommended Citation

Schattke, Jonathan Mark, "A feasibility study of a nuclear power plant with no moving parts" (2016). *Masters Theses*. 7522.  
[http://scholarsmine.mst.edu/masters\\_theses/7522](http://scholarsmine.mst.edu/masters_theses/7522)

This Thesis - Open Access is brought to you for free and open access by Scholars' Mine. It has been accepted for inclusion in Masters Theses by an authorized administrator of Scholars' Mine. This work is protected by U. S. Copyright Law. Unauthorized use including reproduction for redistribution requires the permission of the copyright holder. For more information, please contact [scholarsmine@mst.edu](mailto:scholarsmine@mst.edu).

A FEASIBILITY STUDY OF A NUCLEAR POWER PLANT WITH  
NO MOVING PARTS

by

JONATHAN MARK SCHATTKE

A THESIS

Presented to the Graduate Faculty of the  
MISSOURI UNIVERSITY OF SCIENCE AND TECHNOLOGY

In Partial Fulfillment of the Requirements for the Degree

MASTER OF SCIENCE

IN

NUCLEAR ENGINEERING

2016

Approved by

Xin Liu, Advisor  
Ayodeji B. Alajo  
Joshua P. Schlegel

© 2016

Jonathan Mark Schattke

All Rights Reserved

## ABSTRACT

In a nuclear reactor design, every moving part in a system is considered a failure point. In this study, a proposal is made for designing a nuclear reactor that has no moving parts by coupling an accelerator driven core (removing control system moving parts) to a magnetohydrodynamic generator (removing power generation moving parts) using mercury coolant (removing pumping system moving parts). Further safety is realized by using a subcritical core, where the core is never able to sustain a chain reaction on its own, obviating many safety systems. The design is verified with a Monte Carlo simulation.

## **ACKNOWLEDGMENTS**

I wish to acknowledge the patience of my wife, Laura Warren Schattke, who never stopped believing in me.

## TABLE OF CONTENTS

	Page
ABSTRACT.....	iii
ACKNOWLEDGMENTS.....	iv
LIST OF ILLUSTRATIONS.....	vi
LIST OF TABLES.....	vii
SECTION	
1. INTRODUCTION.....	1
2. THE HIGH FLUX ACCELERATOR.....	4
2.1 MODELING A SPALLATION SYSTEM.....	4
2.2 FINAL CONSIDERATIONS FOR ACCELERATOR.....	6
3. SUBCRITICAL CORE.....	10
3.1 MATERIALS SELECTION.....	10
3.2 MODELING THE CORE.....	12
4. POWER GENERATION.....	17
5. CONCLUSION.....	18
APPENDIX.....	19
BIBLIOGRAPHY.....	25
VITA.....	28

**LIST OF ILLUSTRATIONS**

	Page
Figure 2.1. Layout of core.....	5
Figure 2.2. Neutrons per GeV of beam energy at various proton energies.....	6
Figure 2.3. VASIMR Linear Accelerator.....	9
Figure 3.1. Burndown $k_{eff}$ .....	14
Figure 3.2. Actinide Inventory.....	15

**LIST OF TABLES**

	Page
Table 3.1. Matrix Materials.....	11

## 1. INTRODUCTION

Nuclear power plants have the highest level of safety of any electricity production method developed to date, but are still plagued by public fear of the dangers. Accidents like Chernobyl and Fukushima Daiichi fuel the narrative that nuclear power is dangerous, despite the lack of casualties. A new type of power plant which could be shown to be many times safer would allay these fears and allow the use of the full potential of nuclear energy for the betterment of mankind.

Accelerator Driven Systems (ADS) have the potential for great strides in criticality safety, high level waste disposal, and nonproliferation. By running with a  $k_{eff}$  less than one at all times, the system produces power in the neutron multiplier region, and a cessation of the neutron source leads to reduction (after decay of neutron precursors) of fission to the negligible ambient spontaneous fission level. The level of heat output is directly related to the neutron multiplication factor ( $k_{eff}$ ) of the core and the incoming neutron flux. Since most systems have slightly negative temperature coefficients, the system will automatically reach a steady state power after a slightly higher power warm up, meaning that they are more responsive to load changes than a conventional plant.

The limiting of  $k_{eff}$  to at most 0.995 (for safety considerations with possible breed-up in the fuel) means that the safe maximum fission multiplier is 200, when cold. Each incoming proton in a 1 GeV beam produces  $\sim 25$  neutrons, giving 5000 fissions per proton. Each fission produces 200 MeV (Cochran, 1990), meaning each incoming proton produces 1 TeV, a factor of 1000 on input beam wattage. So to reach Gigawatt class electrical power production, a beam of several Megawatts would be required, which would be prohibitively expensive (the world record proton beam power being the 1.4

MW 580 MeV cyclotron at the Paul Scherrer Institute, with a budget of 250 Million Swiss Francs a year). For this reason the technology lends itself to the Small Modular Reactor (SMR) space. Further consideration must be given to the efficiency of the proton beam; since maximum scientific beam efficiency reaches only 10%, and conventional Rankine cycle power plants in the industry reach about 45% electrical power efficiency, bringing the most powerful accelerator to the highest efficiency would only net 616 MW.

More problematically, most beams have significant downtime, the PSI cyclotron mentioned above hitting 80 hours per week uptime (50%) only rarely. For a power plant, power production must be 99.9% of the time or more (one hour or less down in 6 weeks). Most baseload nuclear plants are currently capable of running the full cycle without shutdown, that is, no unscheduled downtime (there were only 69 scrams in the entire industry in 2013 in the US). Unless an ADS can meet this stringent criteria, it will not be a feasible alternative to conventional nuclear, no matter what advantages it has.

A scientific proton beam requires tight control of proton energy and usually works in pulse mode. A medical imaging or therapeutic device requires tight control of position, beam spread and energy, a 30 degree beam spread would be extremely harmful and the device would be useless for therapy. An ADS proton accelerator requires none of the tight energy, location or beam spread controls; spread the beam 30 degrees and it merely flattens the flux profile. This lower requirement allows accelerators which are more efficient and much cheaper to be designed.

Going to a direct electrical generation system, the capital cost for the plant can be greatly reduced, and reliability increased. By employing magnetohydrodynamic

generators this can be achieved cheaply for high wattage. Power from such a system would be DC, so it would also serve to stabilize the grid.

The scope of this work is a demonstration of feasibility, not full engineering of each component.

## 2. THE HIGH FLUX ACCELERATOR

Existing Accelerator Driven Systems such as the R.A.C.E (Beller, 2004) have used existing scientific beams or specially built scientific beams to produce a neutron source through spallation or photo-neutron interactions. These experiments have demonstrated the multiplication factor of subcritical assemblies, and methods for experimental verification (Jammes, 2007). Drawing 150 Amps at 240 Volts, the RACE-T linear accelerator used 36 kW of power (O’Kelly, 2008). The electron beam produced was just 1.6 kW, an efficiency of just 4.4%. Obviously, a commercial system would hardly be viable if a multiplication factor of 22.5 is required just to break even thermally, and at least 50 is required to break even electrically. Furthermore, they suffered beam losses of 50% even before hitting the target.

An unreliable technology will be completely unsuitable for a commercial plant. The most important considerations are high flux (a large number of particles) and suitable particle energy. A study of what energy would be most efficient must include the cost to accelerate, the results of having a specific energy, and the directionality of the beam and the effect of the beam shape upon the multiplication factor.

### 2.1 MODELING A SPALLATION SYSTEM

MCNP version 6 was used for modeling, since the new high energy physics code is necessary. Figure 2.1 shows the diagram of the system for modeling. In this diagram, green is Mercury, blue is the core material, and red is the iron case. The white outside is air, and it can be assumed there would be no significant reflection from the environment and any particles leaving the outer surface are ignored. The multiple cells in the core are needed to track the evolution of materials in each cell, since little mixing is expected. The

beam is modeled simply as a point source 5 cm above the center and with a directionality uniformly downward. This is not an exact match for the expected source, but allows comparisons.

With spallation on the central liquid mercury column, and counting secondary spallations from the interactions with the heavy metals in the core, runs of at least  $10^6$  protons of various energies generated the data in Figure 2.2, showing the relationship of beam energy to neutrons produced. An energy of at least 25 MeV is needed to spallate

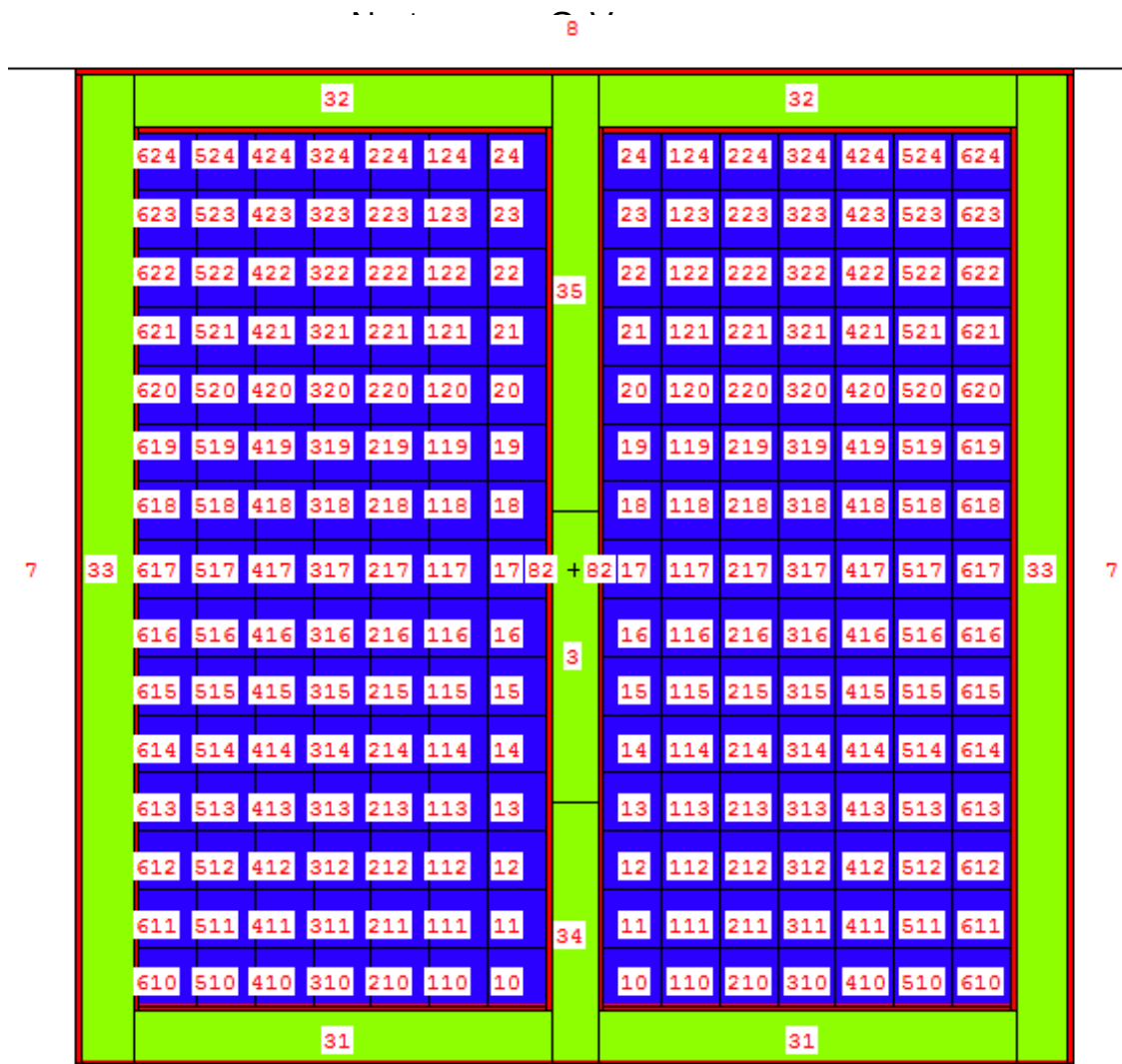


Figure 2.1. Layout of core. Cross section of cylinder.

neutrons off of heavy metal targets (Geurtin, 2005). It is clear that efficacy is linearly related to beam energy, but beam energy is inversely related to efficiency; there would be a “sweet spot” of beam energy where you get the most neutrons per input watt, which will be highly dependent on the accelerator technology used.

## 2.2 FINAL CONSIDERATIONS FOR ACCELERATOR

Ad Astra engineering has been making the VASIMR rocket engine, using ideas pioneered in the early 1980s. The concept is a plasma stream from a magnetic bottle’s center cusp is limited to particle energies at least of a velocity determined by the magnetic field of the constricting coil (see Figure 2.3). By using multiple stages, microwave frequencies can be chosen for each stage to accelerate the particles efficiently for the next stage. The final stage exit magnet strength will determine the particle energy profile at the exit of the device.

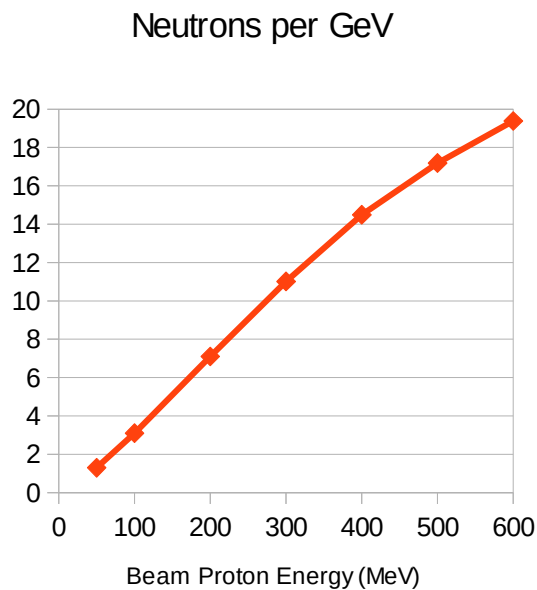


Figure 2.2. Neutrons per GeV of beam energy at various proton energies

The initial plasma formation is in a helicon chamber. Jung (2004) reports being able to reach plasma densities of  $10^{12}$  n/cm. With a 13 kV exciter stage, the velocity is then  $1.1 \times 10^6$  m/s; this then gives  $1.1 \times 10^{11}$  particles per square meter to reach our required flux; this corresponds to  $0.11 \text{ m}^2$ , or 18.9 cm radius, much larger than the device Jung created, but certainly within the realm of engineering. The actual plasma density is dependent on the strength of the magnetic field; Jung found 100 Gauss to be effective, but the exact field strength for best plasma density would have to be determined experimentally. The next stages of the accelerator are magnetic bottles with Cyclotron Resonance Heaters. (VASIMR is a single stage device).

Designing with a modest 300 MeV beam, and choosing magnetic field (B) as 10 T, well within the current state of the art, if  $E=300 \text{ MeV} = 4.8654 \times 10^{-11} \text{ J}$  and  $B=10 \text{ T}$  then

$$\mu = \frac{E}{B} = 4.8654 \times 10^{12} . \quad (1)$$

Since magnetic field to pressure ratio ( $\beta$ ) is

$$\beta = \frac{2En}{B^2 / 2\mu} \quad (2)$$

our  $\beta=1$  limit for n is calculable as

$$n = \frac{B^2 / 2\mu}{2E} = \frac{B^3}{4E^2} = \frac{1 \times 10^3}{4(4.8654 \times 10^{-11})^2} = 1.056 \times 10^{23} \quad (3)$$

which is much more than needed, so the resulting plasma should have a very low  $\beta$  (meaning it can be well confined). Since the density of air is  $1.225 \text{ kg/m}^3$ , this corresponds to 0.11 Torr. If the acceleration begins with atmospheric pressure at room

temperature, ( $\sim 2200$  m/s or 0.025 eV) then the system will have much less than this pressure when the particles are moving at several hundred million eV.

Since the end goal is the best number of neutrons per watt, the system is designed for final energy based upon the efficiency at each energy with a final device. The VASIMR continuous flow axial accelerator achieves 56% efficiency at particle energies in the tens of keV (Longmier 2011), it would be presumptuous to assume a higher energy system could match that in the hundreds of MeV range; but with the Fermi National Accelerator Laboratory confident that they can get a 10% efficient scientific beam in the GeV range, assuming this accelerator design will reach  $\sim 30\%$  efficiency is reasonable.

To have a design total beam energy of 1 MW; 33% efficiency would mean the energy budget for producing the beam is 3 MW. 1 MW beam energy at 300 MeV is a 3.33 mA beam, that is a beam flux of  $2.083 \times 10^{16}$  protons a second, giving rise to  $6.882 \times 10^{16}$  neutrons per second (or  $6.88 \times 10^{10}$  per beam watt). It should also be noted that the beam power is not lost, but is a heat addition to the core coolant.

This will use a mole of mercury every  $10^{10}$  seconds or so. There will likely be the production of helium and tritium in spallation products, a couple moles over the life of the plant. All larger spallation fragments and fission fragments will be sequestered in the sealed design, either dissolved in the mercury or carrier salt, or plating out on the surfaces of the vessel.

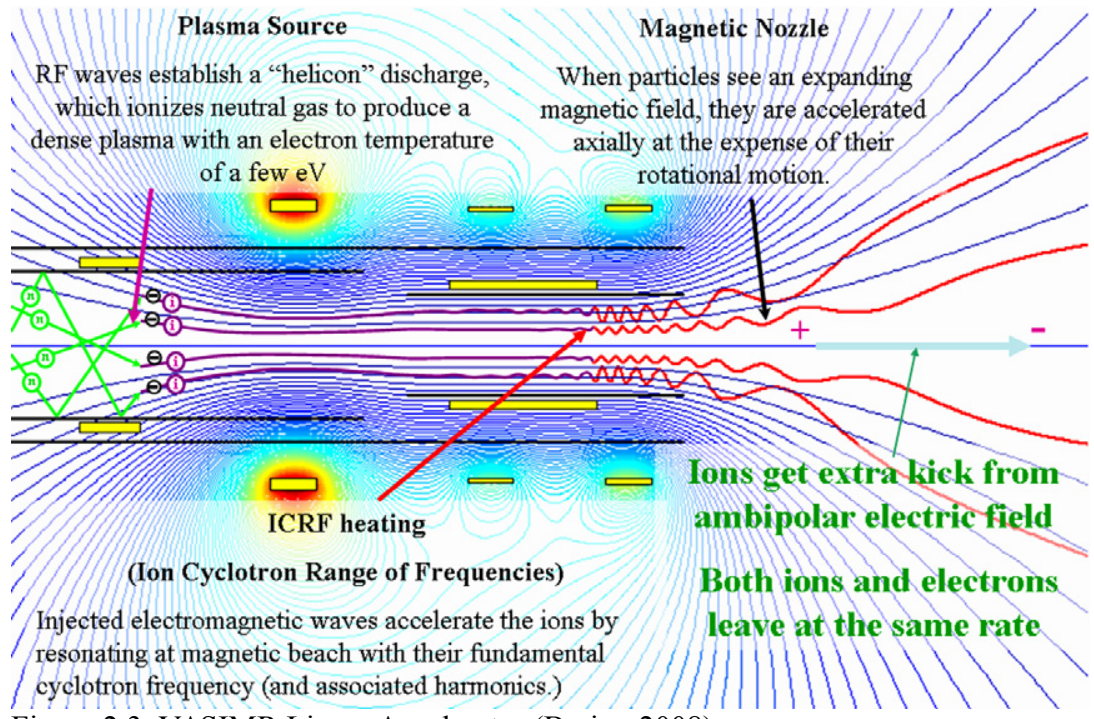


Figure 2.3. VASIMR Linear Accelerator (Bering 2008)

### 3. SUBCRITICAL CORE

Subcritical multiplication occurs in a nuclear reactor when the neutron multiplication factor ( $k_{eff}$ ) is below unity, and the core is exposed to an external source.

This can be expressed as the infinite series

$$n_{tot} = \sum_{j=1}^{\infty} n_0 k_{eff}^j = n_0 \frac{1}{1 - k_{eff}}, \quad (4)$$

this series having a definite solution. Once  $k_{eff}$  goes to unity, an external source will just keep adding neutrons, leading to linear growth, and above unity, the series will exponentially grow to infinity. One of the things a designer of a subcritical system must do is verify the system will not reach criticality under any circumstances.

#### 3.1 MATERIALS SELECTION

A commercially viable small modular reactor must be possible according to the laws of neutron physics, cheap to assemble, made of low priced materials, and demonstrably safe in catastrophic accidents. These criteria drive the choice of candidate materials for the reactor, and the final choice is made on neutronic calculations. Only if the neutronics will not work would a designer revisit the use of exotic or more dangerous materials or more complex construction. The complex assemblies, expensive materials, and dangerous choices made in the operating generation of light water reactors have led to multiple accidents and concomitant monetary losses.

A mercury coolant and spallation target allows the reactor to run at Mercury's 356.58 °C boiling point at atmospheric pressure. By running the thermal cycle at about the same temperature as a LWR but at one atmosphere, the large database of materials science in this temperature realm is usable, and no new exotic materials choices will be

needed. Should a higher temperature be desired, the additional pressure with mercury vapor will be much lower than with water. Mercury is unique as a coolant, as a monatomic gas with a reasonably high boiling point and high density.

The use of economically priced austenitic stainless steel is allowed if the amount of chromium in the neutron flux is kept minima, since chromium is a fairly high cross section material. There are literally decades of experience with stainless steels in all conceivable nuclear environments, including mercury. The same stainless steel will be used for all parts of the system, to avoid any galvanic issues or stresses from differences in thermal expansion rates. This cost will not be prohibitive, because the amount of material to contain a few atmospheres of pressure maximum is minimal (discussion of pressures in the system and thicknesses of piping will be in the power section).

Fluoride salts will corrode stainless steel if the electronegativity of the combining salt is too high, but the corrosive effect is low enough that a few extra millimeters provide years of corrosion protection. However, a solid fluoride salt mix would almost completely relieve corrosion as an issue (as opposed to a molten salt, where atomic motility is great). Table 3.1 shows some relevant properties of candidate salts. The fluoride salt for the matrix, since this is a fast reactor, should not significantly moderate, and should remain stable even at high burnup. The choice of magnesium fluoride was

Table 3.1. Matrix Materials

Material	Atom Density mol/cc	Fast $\sigma_a$	Fast $\sigma_s$
BeF <sub>2</sub>	0.04224	0.0282	14.14
LiF	0.10158	70.71	5.63
MgF <sub>2</sub>	0.05052	0.082	11.42
NaF	0.06092	0.0027	6.79

because magnesium is an alkaline earth metal, with an electronegativity of 1.31. The high reactivity means that any dissociation in the crystal matrix will quickly react with magnesium rather than the steel of the vessel. Other choices are beryllium fluoride, lithium fluoride, or sodium fluoride. It is clear from the large absorption cross section that lithium fluoride would poison the reaction. The higher moderation (scattering cross section) by BeF<sub>2</sub> or LiF means that the system will have a lower steady state fissile content. In MCNP modeling of same-size systems, with same molarity of BeF<sub>2</sub> the  $k_{eff}$  at startup is 0.868 vs. 0.970 for MgF<sub>2</sub> (there is somewhat less mass of salt at the same molarity for BeF<sub>2</sub>), and the breeding is slower in BeF<sub>2</sub> carrier salt.

### 3.2 MODELING THE CORE

MCNP 6 models were used to simulate the core in various configurations, in order to examine characteristics for engineering. CINDER was used for detailed burn calculations to find the production of isotopes not covered by the minimal version included in MCNP. To simulate the action of the beam quickly for MCNP BURN card use, which requires kcode, a rod of plutonium was modeled in the center of the core in order to give the  $k_{eff}$  found with spallation. This approach produces less energetic neutrons, meaning actual experienced fast fissions will be higher and the steady-state <sup>233</sup>U fraction will be slightly higher.

The core of the system is the spallation target area, a 10 cm diameter area of mercury coolant. A simple steel tub containing the subcritical fluoride salt mixture is fastened to the boiler bottom, since it would float on mercury. This tub, of ~1.5 m radius and ~3.0 m height (size determined after several simulation runs to be just subcritical), generates the heat by fission, which is then removed at the surface by the mercury

coolant. A goose-neck vessel contains the liquid mercury, and separates the vapor so that clean dry mercury vapor makes it to power production.

The primary containment is an unpierced high temperature steel tub, welded closed with the entire fissile load for the plant. With breed-up well into the hundreds of Gigawatt days per metric ton, the core is able to be sealed for the service life of the plant. This core must be sized small enough that even when it breeds to steady-state and rests (for the  $^{233}\text{Pa}$  to decay to  $^{233}\text{U}$ ), it will still be certain to be subcritical at all temperatures. The salt mixture will be poured in batches in order to be homogeneous and solid. Some cracking, localized melting during service, or other issues are inconsequential; likewise collection of “hot spots”, stratification, separation of fission products from the matrix and other such effects can be ignored, as long as the surface of the core tub is maintained at a moderate temperature by the mercury. One possible issue would be the collection of fluorine and noble gases in the head space; however, fluorine is very reactive and it is expected that recombination within the matrix will be very robust, especially with the additional protons from beta radiation making the salt less and less stoichiometrically balanced as the fuel burns (fluorine converting to the noble gas neon removes oxidation potential, and magnesium converting to aluminum gains reduction potential)

An initial loading of 8.6% fissile  $^{233}\text{U}$  in fertile Thorium, and 65% molar heavy metal salts leads to a core that is slightly moderated, and the size gives an initial  $k_{eff}$  of 0.987; since the subcritical multiplying factor is  $1/(1-k_{eff})$  this gives 80 fissions per neutron. At a production rate of  $6.88 \times 10^{16}$  neutrons per second, this gives  $5.51282 \times 10^{18}$  fissions; counting 185 MeV recoverable energy per fission, this leads to a core initial heat output of 163 MW(th) from a 1 MW beam at startup.

Figure 3.1 shows the breed-up results as the system runs through various levels of burn. Since breeding is directly related to the fluence, and so is energy output, this is a good measure of core performance. These runs assume only local homogeneity; in actual practice the use of a large volume with only surface cooling would lead to melting of the fluoride salt fuel, which would then set up convection currents and increase mixing.

Figure 3.1 shows the  $k_{eff}$  of a core which is planned as steady state, running 8.6%  $^{233}\text{U}$  and 91.4% Th heavy metal (the Protactinium fraction is very low at this power level, about 0.01%).

At 150 MW from a core of the size used (somewhat larger than a final core must be) there is a heat rate of  $7.08 \text{ MW/m}^3$  and a heat flux of  $3.46 \text{ MW/m}^2$ .

Thermodynamically, the low Peclet number means that the temperature gradient across the liquid metal is very low, so even a moderate pressure rise will assure boiling only at

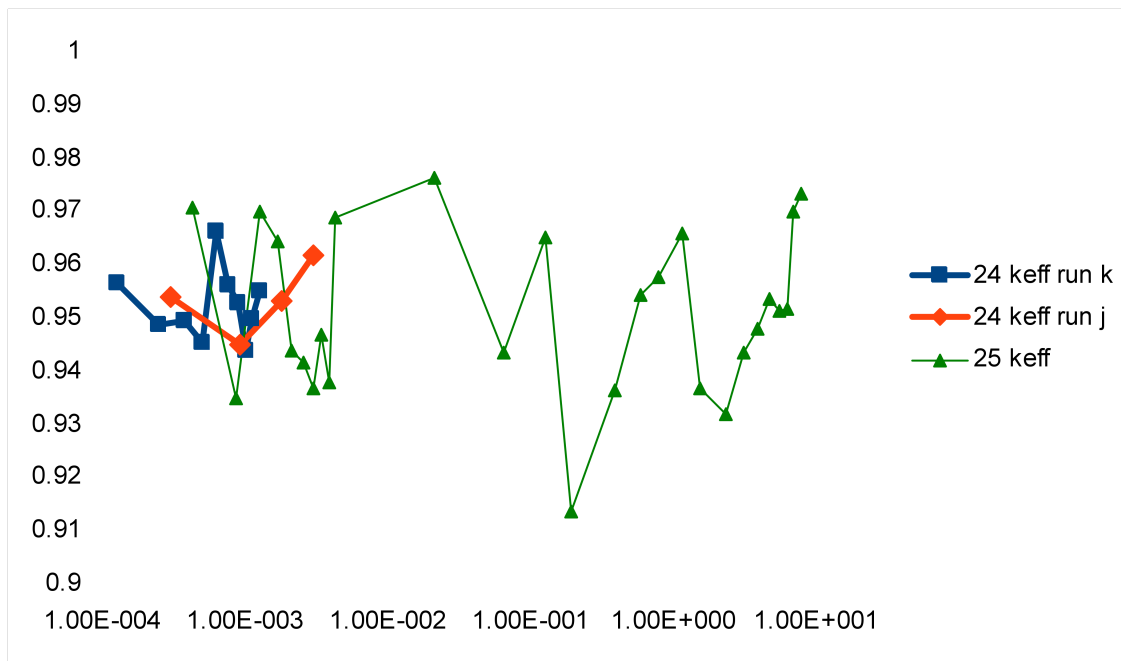


Figure 3.1. Burndown  $k_{eff}$ .

the top surface. Any local boiling in the central column will lower the place where the proton beam strikes, lowering the  $k_{eff}$  of the core, and reducing the heat output. Because of the high density of mercury, the majority of the core is under a pressure of about one atmosphere (since 1 atm=760 mm Hg) With the high heat transfer rate through liquid metal, most of the heat will transfer to a boiling region above the core. Mercury has a specific heat of 0.135 kJ/kg and a heat of vaporization of 61.42 kJ/kg, so 150 MW will boil 2000 kg/sec (7100 tons/hr) from an entering temperature of 250°C. This is about 220 m<sup>3</sup>; at 1200 m/s velocity, this would need a pipe of 0.18 square meters, 24 cm radius.

The demonstration of the strength of the Thorium cycle for in-situ steady state burning is shown in the actinide inventories in Figure 3.2. The plutonium isotopes are in minute concentrations, and the Uranium fissile load climbs slightly during this early part of the burn. Note the <sup>232</sup>U inventory remains small (27 ppm at end of run), which means

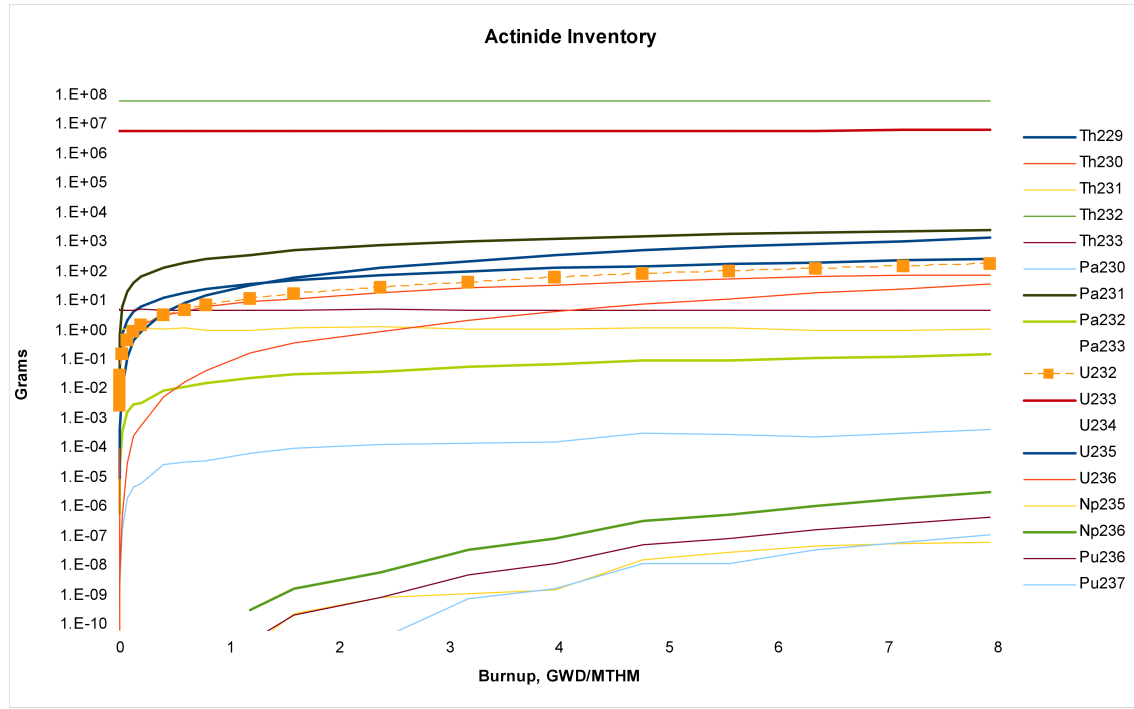


Figure 3.2. Actinide Inventory

the system will have to be rendered proliferation resistant through some other means. Transuranic actinide production in general is minimal, and the waste from this core would be easy to dispose of.

#### 4. POWER GENERATION

Power generation is accomplished with a MHD system. In a disc-type MHD generator, a pair of Helmholtz coils are placed to generate a magnetic field as the plasma flows from the center of a disc to the edge, and the plasma currents then flow around the edge of the disc, allowing the drawing off of the current at opposite sides of the disc directly into electricity with high-temperature contacts.

To generate plasma from mercury steam, another helicon is used. The plasma is then fed directly into the MHD. After power generation, a tube and fin convective flow air cooled heat exchanger neutralizes the plasma and condenses the mercury. Liquid mercury then flows back to the core by gravity.

Coal plant MHD generators with plasmas that have fairly high neutral percentages have reached 20% efficiency; while fully ionized systems should reach much higher efficiency, for the purposes of energy balance, assuming 20% is reasonable. The 150 MW(th) then produces 30 MWe.

Mercury steam from the nuclear boiler at 2 atmospheres pressure (400°C, 210 kpa, 41.661 kJ/kg) is swirled through a droplet separator to have clean, dry steam enter the power equipment. This then goes through a Helicon to ionize it (first ionization energy is 10.43 eV) and then into our MHD. The steam then goes through a fin and tube condenser to bring it below boiling, back to 250°C (10 kpa, 34.42 kJ/kg). This pressure differential assures good steam flow at all times. Each kilogram of mercury in this system has 7.2 kJ of enthalpy available; for this level of feasibility, we assume perfect regeneration of the enthalpy from the exit side of the MHD to the condensed cold mercury.

## 5. CONCLUSION

The advantages in safety of a fully sealed nuclear power plant with no moving parts are manifest and great. Each of the parts of this reactor design is feasible, within current state of the art, and using no exotic materials. The most important part of the reactor, with the most research being needed, is the high flux low price accelerator, but even a retired medical imaging cyclotron could be used to demonstrate the concept.

## APPENDIX

## MCNP CODE

```

ThorMer Preliminary Version 2
c The Thorium Mercury ADEP
c Jonathan Schattke 9/27/13
c Run 04: neutron source information
c Run04a: adjust target area
c Run05a: mock point source, kcode - FAIL
c Run05b: mock point source, kcode 1 cycle burn - FAIL
c Run06: attempt to get MCNP to produce fission product list
c         and neutron spectrum in fuel
c Run06a: get fuller product list
c Run07: k_eff at 1% U233
c Run07a: k_eff at 2% U233
c Run07b: k_eff at 3% U233
c Run07c: k_eff at 4% U233
c Run07d: k_eff at 5% U233
c Run07e: k_eff at 6% U233
c Run07f: k_eff at 7% U233
c Run07g: k_eff at 8% U233
c Run07h: k_eff at 9% U233
c Run07j: k_eff at 8.12% U233, expected steady state
c Run08: Radial Spatial distribution of fission at 8.12% Homogeneous
c Run08b: Radial Spatial distribution of fission at 0%
c Run09: Axial Spatial distribution of fission at 0%
c Run09a: Axial and radial distribution of fission, 0%
c Run10: axial and radial distribution, flux enhancement w/ Natural Uranium
c Run11: axial and radial distribution, BeF2 salt
c Run12: distribution, ThN:(MgF2)2
c Run13: axial and radial distribution, flux enhancement w/ Natural Uranium,
ThF4:(MgF2)2, breed step 1
c Run14: a&r dist, UF4 first ring, ThF4/MgF2 balance
c Run15: a&r dist, 5% enriched UF4 first ring
c Run16: a&r dist, 5% enriched UF4 first 2 rings, t0
c Run17: a&r dist, 5% enriched UF4 first 2 rings, t1 (~0.5%)
c Run18: a&r dist, 5% enriched UF4 t0
c Run19: a&r CINDER, (5% PuF4/95% ThF4):1 MgF2:1
c Run20: a&r dist, simplified rings
c Run21: a&r as above, 5%enriched U
c Run22: a&r as 20, BeF moderator
c Run23: adjust size to assure no keff>1 possible
c Run24: adjust size, start at expected steady state U233
c Run24a: adjust size to 60cm, start at expected steady state (8.6%)
c Run24b,c,d,e: more sizes, increasing sizes 70,80,85,95
c Run24f: 95cm 500MeV verify same k_eff
c Run24g,h: 120cm 300MeV, 150cm
c Run24j,k,m: characterization of 150cm core keff over startup
c Run25: increase HM molarity to increase keff
c
c cells
10 10 -4.85 10 -11 110 -111 vol=4.71239E+04
11 11 -4.85 10 -11 111 -112 vol=1.25664E+04
12 12 -4.85 10 -11 112 -113 vol=6.28319E+03
13 13 -4.85 10 -11 113 -114 vol=6.28319E+03
14 14 -4.85 10 -11 114 -115 vol=6.28319E+03
15 15 -4.85 10 -11 115 -116 vol=6.28319E+03
16 16 -4.85 10 -11 116 -117 vol=6.28319E+03
17 17 -4.85 10 -11 117 -121 vol=6.28319E+03
18 18 -4.85 10 -11 121 -122 vol=6.28319E+03
19 19 -4.85 10 -11 122 -123 vol=6.28319E+03
20 20 -4.85 10 -11 123 -124 vol=6.28319E+03
21 21 -4.85 10 -11 124 -125 vol=6.28319E+03
22 22 -4.85 10 -11 125 -126 vol=6.28319E+03
23 23 -4.85 10 -11 126 -127 vol=1.25664E+04
24 24 -4.85 10 -11 127 -130 vol=4.71239E+04
110 110 -4.85 11 -12 110 -111 vol=9.42478E+04

```

```

111 111 -4.85 11 -12 111 -112 vol=2.51327E+04
112 112 -4.85 11 -12 112 -113 vol=1.25664E+04
113 113 -4.85 11 -12 113 -114 vol=1.25664E+04
114 114 -4.85 11 -12 114 -115 vol=1.25664E+04
115 115 -4.85 11 -12 115 -116 vol=1.25664E+04
116 116 -4.85 11 -12 116 -117 vol=1.25664E+04
117 117 -4.85 11 -12 117 -121 vol=1.25664E+04
118 118 -4.85 11 -12 121 -122 vol=1.25664E+04
119 119 -4.85 11 -12 122 -123 vol=1.25664E+04
120 120 -4.85 11 -12 123 -124 vol=1.25664E+04
121 121 -4.85 11 -12 124 -125 vol=1.25664E+04
122 122 -4.85 11 -12 125 -126 vol=1.25664E+04
123 123 -4.85 11 -12 126 -127 vol=2.51327E+04
124 124 -4.85 11 -12 127 -130 vol=9.42478E+04
210 210 -4.85 12 -14 110 -111 vol=3.29867E+05
211 211 -4.85 12 -14 111 -112 vol=8.79646E+04
212 212 -4.85 12 -14 112 -113 vol=43982.3
213 213 -4.85 12 -14 113 -114 vol=43982.3
214 214 -4.85 12 -14 114 -115 vol=43982.3
215 215 -4.85 12 -14 115 -116 vol=43982.3
216 216 -4.85 12 -14 116 -117 vol=43982.3
217 217 -4.85 12 -14 117 -121 vol=43982.3
218 218 -4.85 12 -14 121 -122 vol=43982.3
219 219 -4.85 12 -14 122 -123 vol=43982.3
220 220 -4.85 12 -14 123 -124 vol=43982.3
221 221 -4.85 12 -14 124 -125 vol=43982.3
222 222 -4.85 12 -14 125 -126 vol=43982.3
223 223 -4.85 12 -14 126 -127 vol=8.79646E+04
224 224 -4.85 12 -14 127 -130 vol=3.29867E+05
410 410 -4.85 14 -20 110 -111 vol=4.82431E+06
411 411 -4.85 14 -20 111 -112 vol=1.28648E+06
412 412 -4.85 14 -20 112 -113 vol=6.43241E+05
413 413 -4.85 14 -20 113 -114 vol=6.43241E+05
414 414 -4.85 14 -20 114 -115 vol=6.43241E+05
415 415 -4.85 14 -20 115 -116 vol=6.43241E+05
416 416 -4.85 14 -20 116 -117 vol=6.43241E+05
417 417 -4.85 14 -20 117 -121 vol=6.43241E+05
418 418 -4.85 14 -20 121 -122 vol=6.43241E+05
419 419 -4.85 14 -20 122 -123 vol=6.43241E+05
420 420 -4.85 14 -20 123 -124 vol=6.43241E+05
421 421 -4.85 14 -20 124 -125 vol=6.43241E+05
422 422 -4.85 14 -20 125 -126 vol=6.43241E+05
423 423 -4.85 14 -20 126 -127 vol=1.28648E+06
424 424 -4.85 14 -20 127 -130 vol=4.82431E+06
c 70 9 -19.8 -9 210 -200
70 50 -13.6 -9 210 -200
80 100 -7.8 40 -10 100 -111
81 100 -7.8 40 -10 111 -112
82 100 -7.8 40 -10 112 -113
83 100 -7.8 40 -10 113 -114
84 100 -7.8 40 -10 114 -115
85 100 -7.8 40 -10 115 -116
86 100 -7.8 40 -10 116 -117
87 100 -7.8 40 -10 117 -121
88 100 -7.8 40 -10 121 -122
89 100 -7.8 40 -10 122 -123
90 100 -7.8 40 -10 123 -124
91 100 -7.8 40 -10 124 -125
92 100 -7.8 40 -10 125 -126
93 100 -7.8 40 -10 126 -127
94 100 -7.8 40 -10 127 -130
95 100 -7.8 20 -30 -130 100
96 100 -7.8 10 -20 -130 120
97 100 -7.8 10 -20 -110 100
3 50 -13.6 210 -200 9 -40
3.1 50 -13.6 140 -100 40 -30
3.2 50 -13.6 130 -160 40 -30
3.3 50 -13.6 140 -160 30 -50
3.4 50 -13.6 140 -210 -40
3.5 50 -13.6 200 -160 -40
4 100 -7.8 140 -160 50 -60
4.1 100 -7.8 160 -170 -60

```

```

4.2 100 -7.8 150 -140 -60
5 0 -150
7 0 60 150 -170
8 0 170

```

```
c surfaces
```

```
c 10 series: cylinders
```

```
9 cz 2.05
```

```
10 cz 5
```

```
11 cz 15
```

```
12 cz 25
```

```
13 cz 35
```

```
14 cz 45
```

```
15 cz 55
```

```
16 cz 75
```

```
20 cz 150
```

```
30 cz 151
```

```
40 cz 4
```

```
50 cz 161
```

```
60 cz 162
```

```
c 100 series: xy planes
```

```
100 pz -151
```

```
110 pz -150
```

```
111 pz -75
```

```
112 pz -55
```

```
113 pz -45
```

```
114 pz -35
```

```
115 pz -25
```

```
116 pz -15
```

```
117 pz -5
```

```
120 pz 151
```

```
121 pz 5
```

```
122 pz 15
```

```
123 pz 25
```

```
124 pz 35
```

```
125 pz 45
```

```
126 pz 55
```

```
127 pz 75
```

```
130 pz 150
```

```
140 pz -161
```

```
150 pz -162
```

```
160 pz 161
```

```
170 pz 162
```

```
c 200 series: tally cell surfaces
```

```
200 pz 10
```

```
210 pz -30
```

```
phys:n 1000
```

```
c phys:p 1000
```

```
mphys
```

```
mode N $ H P / D T S A
```

```
imp:N,H,/,D,T,S,A 1 87R 0 0 0
```

```
nps 1e5
```

```
c imp:N 1 87R 0 0 0
```

```
c kcode 10000 0.946 15 65
```

```
c BURN &
```

```
c TIME= 0.2 0.2 0.2 0.2 0.2 0.2 0.2 0.2 0.2 0.2 & 8 20 30 30 92 90 92 &
```

```
c 182 184 364 366 364 366 364 366 364 366 & $ ..1m .1q ..1y .
```

```
2y ..5y ....10y
```

```
c LATER: PFRAC with each step having maximum power for a 1 MW beam at the k_eff
```

```
c POWER= 40.0 &
```

```
c MAT 10 11 12 13 14 15 16 17 18 19 20 21 22 23 24 &
```

```
c 110 111 112 113 114 115 116 117 118 119 120 121 122 123 124 &
```

```
c 210 211 212 213 214 215 216 217 218 219 220 221 222 223 224 &
```

```
c 410 411 412 413 414 415 416 417 418 419 420 421 422 423 424 &
```

```
c AFMIN=1e-16 &
```

```
c BOPT 1.0 -24 1.0
```

```
c Materials
```

```
c m9 Criticality source to simulate beam, Pu
```

```
m9 94239 1
```

```
c 10 series: fuel (5%Pu,95%Th)F4/MgF2
```

```
c Mat'l Density fraction
```

c	UF4	6.59331	0.05375	0.28351	124204
c	ThF4	6.3	0.57125	2.9925	
c	MgF2	3.148	0.375	1.574	
c				4.85001	124204
m10	92233	.086	90232	.914	
	9019	5.2			
	12024	0.47394	12025	0.06	12026 0.06606
m11	92233	.086	90232	.914	
	9019	5.2			
	12024	0.47394	12025	0.06	12026 0.06606
m12	92233	.086	90232	.914	
	9019	5.2			
	12024	0.47394	12025	0.06	12026 0.06606
m13	92233	.086	90232	.914	
	9019	5.2			
	12024	0.47394	12025	0.06	12026 0.06606
m14	92233	.086	90232	.914	
	9019	5.2			
	12024	0.47394	12025	0.06	12026 0.06606
m15	92233	.086	90232	.914	
	9019	5.2			
	12024	0.47394	12025	0.06	12026 0.06606
m16	92233	.086	90232	.914	
	9019	5.2			
	12024	0.47394	12025	0.06	12026 0.06606
m17	92233	.086	90232	.914	
	9019	5.2			
	12024	0.47394	12025	0.06	12026 0.06606
m18	92233	.086	90232	.914	
	9019	5.2			
	12024	0.47394	12025	0.06	12026 0.06606
m19	92233	.086	90232	.914	
	9019	5.2			
	12024	0.47394	12025	0.06	12026 0.06606
m20	92233	.086	90232	.914	
	9019	5.2			
	12024	0.47394	12025	0.06	12026 0.06606
m21	92233	.086	90232	.914	
	9019	5.2			
	12024	0.47394	12025	0.06	12026 0.06606
m22	92233	.086	90232	.914	
	9019	5.2			
	12024	0.47394	12025	0.06	12026 0.06606
m23	92233	.086	90232	.914	
	9019	5.2			
	12024	0.47394	12025	0.06	12026 0.06606
m24	92233	.086	90232	.914	
	9019	5.2			
	12024	0.47394	12025	0.06	12026 0.06606
m110	92233	.086	90232	.914	
	9019	5.2			
	12024	0.47394	12025	0.06	12026 0.06606
m111	92233	.086	90232	.914	
	9019	5.2			
	12024	0.47394	12025	0.06	12026 0.06606
m112	92233	.086	90232	.914	
	9019	5.2			
	12024	0.47394	12025	0.06	12026 0.06606
m113	92233	.086	90232	.914	
	9019	5.2			
	12024	0.47394	12025	0.06	12026 0.06606
m114	92233	.086	90232	.914	
	9019	5.2			
	12024	0.47394	12025	0.06	12026 0.06606
m115	92233	.086	90232	.914	
	9019	5.2			
	12024	0.47394	12025	0.06	12026 0.06606
m116	92233	.086	90232	.914	
	9019	5.2			
	12024	0.47394	12025	0.06	12026 0.06606
m117	92233	.086	90232	.914	
	9019	5.2			

m118	12024	0.47394	12025	0.06	12026	0.06606
	92233	.086	90232	.914		
	9019	5.2				
m119	12024	0.47394	12025	0.06	12026	0.06606
	92233	.086	90232	.914		
	9019	5.2				
m120	12024	0.47394	12025	0.06	12026	0.06606
	92233	.086	90232	.914		
	9019	5.2				
m121	12024	0.47394	12025	0.06	12026	0.06606
	92233	.086	90232	.914		
	9019	5.2				
m122	12024	0.47394	12025	0.06	12026	0.06606
	92233	.086	90232	.914		
	9019	5.2				
m123	12024	0.47394	12025	0.06	12026	0.06606
	92233	.086	90232	.914		
	9019	5.2				
m124	12024	0.47394	12025	0.06	12026	0.06606
	92233	.086	90232	.914		
	9019	5.2				
m210	12024	0.47394	12025	0.06	12026	0.06606
	92233	.086	90232	.914		
	9019	5.2				
m211	12024	0.47394	12025	0.06	12026	0.06606
	92233	.086	90232	.914		
	9019	5.2				
m212	12024	0.47394	12025	0.06	12026	0.06606
	92233	.086	90232	.914		
	9019	5.2				
m213	12024	0.47394	12025	0.06	12026	0.06606
	92233	.086	90232	.914		
	9019	5.2				
m214	12024	0.47394	12025	0.06	12026	0.06606
	92233	.086	90232	.914		
	9019	5.2				
m215	12024	0.47394	12025	0.06	12026	0.06606
	92233	.086	90232	.914		
	9019	5.2				
m216	12024	0.47394	12025	0.06	12026	0.06606
	92233	.086	90232	.914		
	9019	5.2				
m217	12024	0.47394	12025	0.06	12026	0.06606
	92233	.086	90232	.914		
	9019	5.2				
m218	12024	0.47394	12025	0.06	12026	0.06606
	92233	.086	90232	.914		
	9019	5.2				
m219	12024	0.47394	12025	0.06	12026	0.06606
	92233	.086	90232	.914		
	9019	5.2				
m220	12024	0.47394	12025	0.06	12026	0.06606
	92233	.086	90232	.914		
	9019	5.2				
m221	12024	0.47394	12025	0.06	12026	0.06606
	92233	.086	90232	.914		
	9019	5.2				
m222	12024	0.47394	12025	0.06	12026	0.06606
	92233	.086	90232	.914		
	9019	5.2				
m223	12024	0.47394	12025	0.06	12026	0.06606
	92233	.086	90232	.914		
	9019	5.2				
m224	12024	0.47394	12025	0.06	12026	0.06606
	92233	.086	90232	.914		
	9019	5.2				
m410	12024	0.47394	12025	0.06	12026	0.06606
	92233	.086	90232	.914		
	9019	5.2				
m411	12024	0.47394	12025	0.06	12026	0.06606
	92233	.086	90232	.914		
	9019	5.2				

```

m412 12024 0.47394 12025 0.06 12026 0.06606
      92233 .086 90232 .914
      9019 5.2
m413 12024 0.47394 12025 0.06 12026 0.06606
      92233 .086 90232 .914
      9019 5.2
m414 12024 0.47394 12025 0.06 12026 0.06606
      92233 .086 90232 .914
      9019 5.2
m415 12024 0.47394 12025 0.06 12026 0.06606
      92233 .086 90232 .914
      9019 5.2
m416 12024 0.47394 12025 0.06 12026 0.06606
      92233 .086 90232 .914
      9019 5.2
m417 12024 0.47394 12025 0.06 12026 0.06606
      92233 .086 90232 .914
      9019 5.2
m418 12024 0.47394 12025 0.06 12026 0.06606
      92233 .086 90232 .914
      9019 5.2
m419 12024 0.47394 12025 0.06 12026 0.06606
      92233 .086 90232 .914
      9019 5.2
m420 12024 0.47394 12025 0.06 12026 0.06606
      92233 .086 90232 .914
      9019 5.2
m421 12024 0.47394 12025 0.06 12026 0.06606
      92233 .086 90232 .914
      9019 5.2
m422 12024 0.47394 12025 0.06 12026 0.06606
      92233 .086 90232 .914
      9019 5.2
m423 12024 0.47394 12025 0.06 12026 0.06606
      92233 .086 90232 .914
      9019 5.2
m424 12024 0.47394 12025 0.06 12026 0.06606
      92233 .086 90232 .914
      9019 5.2
m50 80000 1
c 100 series: structure Fe
m100 26054 0.058
      26056 0.9172
      26057 0.022
      26058 0.0028
sdef erg=300 pos=0 0.1 10 vec=0 0 -1 dir=1 axs 0 0 -1 rad d1 ext 0
sil 24.5
spl -21
FC4 Neutron flux in fuel and beam collision region
F4:n 3 10 11 12 13 14 15 16 17 18 19 20 21 22 23 24 &
     110 111 112 113 114 115 116 117 118 119 120 121 122 123 124 &
     210 211 212 213 214 215 216 217 218 219 220 221 222 223 224 &
     410 411 412 413 414 415 416 417 418 419 420 421 422 423 424 &
     80 81 82 84 84 85 86 87 88 89 90 91 92 93 94
e4 5.00000e-09 1.00000e-08 1.50000e-08 2.00000e-08 2.50000e-08 3.00000e-08
     3.50000e-08 4.20000e-08 5.00000e-08 5.80000e-08 6.70000e-08 8.00000e-08
     1.00000e-07 1.52000e-07 2.51000e-07 4.14000e-07 6.83000e-07 1.12500e-06
     1.85500e-06 3.05900e-06 5.04300e-06 8.31500e-06 1.37100e-05 2.26000e-05
     3.72700e-05 6.14400e-05 1.01300e-04 1.67000e-04 2.75400e-04 4.54000e-04
     7.48500e-04 1.23400e-03 2.03500e-03 2.40400e-03 2.84000e-03 3.35500e-03
     5.53100e-03 9.11900e-03 1.50300e-02 1.98900e-02 2.55400e-02 4.08700e-02
     6.73800e-02 1.11100e-01 1.83200e-01 3.02000e-01 3.88700e-01 4.97900e-01
     6.39279e-01 8.20850e-01 1.10803e+00 1.35335e+00 1.73774e+00 2.23130e+00
     2.86505e+00 3.67879e+00 4.96585e+00 6.06500e+00 1.00000e+01 1.49182e+01
     1.69046e+01 2.00000e+01 2.50000e+01 t
print 20 40 50 60 70 72 98 100 102 110 126 120 130 140 160
      161 162 190 200

```

## BIBLIOGRAPHY

- Azevedo, C.R.F. "Selection of Cladding Material for Nuclear Fission Reactors," *Eng Fail Anal* (2011).
- Beller, Dennis, "Overview of the AFCI Reactor-Accelerator Coupling Experiments (RACE) Project." Idaho Accelerator Center, 2004.
- Bergman, Theodore L., Adrienne S. Lavine, Frank P. Incropera, and David P. Dewitt. *Introduction to Heat Transfer*. 6<sup>th</sup> Ed. John Wiley and Sons, 2007.
- Bering, E.A., F.R. Chang-Diaz, J.P. Squire, M. Brukardt, T.W. Glover, R.D. Bengtson, V.T. Jacobson, G.E. McCaskill, L. Cassady, "Electromagnetic Ion Cyclotron Resonance Heating in the VASIMR," *Advances in Space Research* 42 (2008) 192–205.
- Carter, M.D., F.W. Betty, Jr., G.C. Barber, R.H. Goulding, Y. Mori, D.O. Sparks, K.F. White, E.F. Jaeger, F.R. Chang-Diaz, J.P. Squire, "Comparing Experiments with Modeling for Light Ion Helicon Plasma Sources," *Phy. Plasmas*, Vol. 9, No. 12 (2002) 5097-5110.
- Chen, Francis F. *Introduction to Plasma Physics and Controlled Fusion*. 2<sup>nd</sup> Ed. New York: Plenum Press, 1984.
- Cochran, Robert G. and Nicholas Tsoulfanidis. *The Nuclear Fuel Cycle: Analysis and Management*. 2<sup>nd</sup> Ed. LaGrange Park, IL: American Nuclear Society, 1990.
- Dunderstadt, James J. and Louis J. Hamilton. *Nuclear Reactor Analysis*. John Wiley and Sons, 1976.
- Fermi National Accelerator Laboratory, Batavia, IL. *Very Big Accelerators as Energy Producers*, R.R. Wilson, 1976.
- Geurtin, A., N. Marie, S. Auduc, V. Blideanu, Th. Delbar, P Eudes, Y. Foucher, F. Haddad, T. Kirchner, Ch. Le Brun, C. Lebrun, F.R. Lecolley, X. Ledoux, F. Lefèbvres, T. Lefort, M. Louvel, A. Ninane, Y. Patin, Ph. Pras, G. Rivière, C. Varignon, "Neutron and light-charged-particle productions in proton-induced reactions on <sup>208</sup>Pb at 62.9 MeV," *Eur. Phys. J. A*. 23 (2005), 49-60.
- Goddard Space Flight Center, Greenbelt, MD. *Review of Liquid-Metal Magnetohydrodynamic Energy Conversion Cycles*, Frederick H. Morse.
- Gudowski, Waclaw, "Accelerator-driven Transmutation Projects. The Importance of Nuclear Physics Research for Waste Transmutation," *Nuclear Physics A* 654 (1999), 436c-457c.

- Gohar, Yousry, David Johnson, Todd Johnson, Shekhar Mishra, "Fermilab Project-X Nuclear Energy Application Accelerator, Spallation Target and Transmutation Technology Demonstration."
- Ignatovich, Vladimir K., "Fundamental Neutron Research in JINR (Dubna)," 1996.
- JAMMES, C., D.E. Beller, K. Sabourov, E. Stankovskiy, F. Harmon, K. Folkman, "Experimental results of the RACE-ISU international collaboration on ADS." In Int. Conf. AccApp'07, 2007.
- Jung, H.D., M.J. Park, S.H. Kim, and Y.S. Hwang, "Development of a Compact Helicon Ion Source for Neutron Generators," Rev. Sci. Instrum., vol. 75, no. 5 (2004), 1878-1880.
- Kim, G., D. May, P. McIntyre, A. Sattarov, "A Superconducting Isochronous Cyclotron Stack as a Driver for a Thorium-Cycle Power Reactor," Proceedings of the 2001 Particle Accelerator Conference, Chicago (2001) 2593-2595.
- Lamarsh, John R. and Anthony J. Baratta. Introduction to Nuclear Engineering. 3<sup>rd</sup> Ed. Upper Saddle River, NJ: Prentice Hall, 2001.
- LAMPF User's Group Workshop, Washington, DC April 20, 1994. An Overview of Accelerator-Driven Transmutation Technology, Whitepaper submitted by Edward A. Heighway.
- Li, Kam W. and A. Paul Priddy. Power Plant System Design. John Wiley and Sons, 1985.
- Longmier, Benjamin W., Leonard D. Cassady, Maxwell G. Ballenger, Mark D. Carter, Franklin R. Chang-Díaz, Tim W. Glover, Andrew V. Ilin, Greg E. McCaskill, Chris S. Olsen, and Jared P. Squire, Edgar A. Bering III, "VX-200 Magnetoplasma Thruster Performance Results Exceeding Fifty-Percent Thruster Efficiency," Journal of Propulsion and Power, Vol. 27, No. 4, July–August 2011.
- Longmier, Benjamin W., Jared P. Squire, Mark D. Carter, Leonard D. Cassady, Tim W. Glover, William J. Chancery, Chris S. Oliver, Andrew V. Ilin, Greg E. McCaskill, Franklin R. Chang-Diaz, Edgar A. Bering III, "Ambipolar Ion Acceleration in the Expanding Magnetic Nozzle of the VaASIMR VX-200i," 45<sup>th</sup> ASIA/ASME/ASE/ASEE Joint Propulsion Conference & Exhibit, 2005.
- Munson, Bruce R., Donald F. Young, Theodore H. Okiishi and Wade W. Huebsch. Fundamentals of Fluid Mechanics. 6<sup>th</sup> Ed. John Wiley and Sons, 2009.
- Magill, J., P. Peerani and J. van Geel, "Basic Aspects of Sub-Critical Systems Using Thin Fissile Layers," European Commission Joint Research Centre, Institute for Transuranium Elements, Karlsruhe, Germany.

- O'Kelly, D.S. "Operation and Reactivity Measurements of an Accelerator Driven Subcritical TRIGA Reactor." The University of Texas at Austin, Mechanical Engineering, 2008.
- Olander, D. "Nuclear Fuels – Present and Future," Journal of Nuclear Materials (2009) 1-22.
- Rubbia, Carlo, "Sub Critical Thorium Reactors," Energy 2050, CERN, Geneva, Switzerland (2009).
- Satyamurthy, P., S.B. Deqwekar, and P.K. Nema, "Design of a Molten Heavy-Metal Coolant and Target for Fast-Thermal Accelerator Driven Sub-Critical System (ADS)," Bhabha Atomic Research Centre, Mumbai, India (2003).
- Sheehan, J.P., B.W. Longmier, E.A. Bering, C.S. Olsen, J.P. Squire, M.G. Bellenger, M.D. Carter, L.D. Cassady, F.R. Chang Diaz, T.W. Glower, A.V. Illin, "Temperature Gradients due to Adiabatic Plasma Expansion in a Magnetic Nozzle," Plasma Sources Sci. Technol. 23 (2014) 045014 (7pp).
- Shultis, J. Kenneth and Richard E. Faw. Fundamentals of Nuclear Science and Engineering. 2<sup>nd</sup> Ed. Boca Raton, FL: CRC Press, 2008.
- Smith, Blair, Knight, Travis W., and Anghaie, Samin, "Overview of Nuclear MHD Conversion for Multi-Megawatt Electric Propulsion," CP552, Space Technology and Applications International Forum-2001, American Institute of Physics 2001.
- Steinberg, M., "The Spallator and APEX Nuclear Fuel Cycle: A New Option for Nuclear Power," IEEE Trans. On Nuc. Power, Vol NS-30, No 1 (1983), 14-19.
- Takeshita, Shinji, Chainarong Buttapeng, Nob. Harada. "Characteristics of Plasma Produced by MHD Technology and its Application to Propulsion Systems," Vacuum 84 (2010), 685-688.
- Todreas, Neil E. and Mujid S. Kazimi. Nuclear Systems, vol. 1 Thermal Hydraulic Fundamentals. 2<sup>nd</sup> Ed. Boca Raton, FL: CRC Press, 2012.
- Welty, James R., Charles E. Wicks, Robert E. Wilson and Gregory L. Rorrer. Fundamentals of Momentum, Heat, and Mass Transfer. 5<sup>th</sup> Ed. John Wiley and Sons, 2008.
- Wider, H.U., J. Karlsson and JRC Ispra, "Safety Aspects of Heavy-Metal-Cooled Accelerator-Driven Waste Burners," Proceedings of Workshop on Innovative Options in the Field of Nuclear Fission Energy, Les Houches, France, April 27-May 1, 1998.

## VITA

Jonathan Schattke received his Bachelor of Science in Nuclear Engineering from Missouri University of Science and Technology in December of 2013.

He received his Master of Science in Nuclear Engineering from the Missouri University of Science and Technology in May of 2016.

He has been a Programmer/Analyst, a Design Draftsman, and a HVAC Engineer.